A Subdivision Algorithm for the Computation of Unstable Manifolds and Global Attractors

Michael Dellnitz*
Inst für Angewandte Mathematik
Universität Hamburg
D-20146 Hamburg
Germany

Andreas Hohmann†
Konrad-Zuse-Zentrum für
Informationstechnik Berlin
D-10711 Berlin
Germany

May 3, 1995

Summary

Each invariant set of a given dynamical system is part of the global attractor. Therefore the global attractor contains all the potentially interesting dynamics, and, in particular, it contains every (global) unstable manifold. For this reason it is of interest to have an algorithm which allows to approximate the global attractor numerically. In this article we develop such an algorithm using a subdivision technique. We prove convergence of this method in a very general setting, and, moreover, we describe the qualitative convergence behavior in the presence of a hyperbolic structure. The algorithm can successfully be applied to dynamical systems of moderate dimension, and we illustrate this fact by several numerical examples.

Mathematics Subject Classification (1991): 65L05, 65L70, 58F15, 58F12.

*Research supported in part by the Deutsche Forschungsgemeinschaft, ONR Grant N00014-94-1-0317 and the Konrad-Zuse-Zentrum für Informationstechnik Berlin.

†Research supported by the Deutsche Forschungsgemeinschaft.

1 Introduction

It is well known that unstable manifolds of invariant sets have a crucial influence on the complexity of the dynamical behavior which is present in a given dynamical system. For instance,

- a transverse intersection of an unstable manifold with a stable manifold leads to the existence of complicated dynamical behavior close to this intersection;
- frequently attracting sets coincide with the closure of unstable manifolds of hyperbolic periodic points;
- another important example is provided by homoclinic tangencies of stable and unstable manifolds. These also lead to extremely rich dynamical behavior.

These are just a few examples. For a more detailed exposition and for an overview on this subject the reader is referred to [4, 12].

The mathematical object which contains all the unstable manifolds is the *global attractor*. Roughly speaking, the global attractor is defined to be the set which is eventually approached by every orbit of the underlying dynamical system. In particular, the global attractor contains all the ω-limit sets.

In this paper we propose a new algorithm for the efficient approximation of parts of the global attractor — namely of so-called *relative global attractors* (see §2) — including unstable manifolds. The existing methods for the computation of unstable manifolds operate *locally* in the sense that one starts the computation at a hyperbolic periodic point and then computes part of the unstable manifold by some sort of continuation procedure (see e.g. [13, 16]). In contrast to these methods, we propose a *global* approach using an adaptive subdivision process.

Let us be more precise. Suppose that the dynamical system is defined on R^n. We start by specifying a box in R^n in which we want to analyze the dynamical behavior. In a first step we subdivide this box and throw away boxes which do not contain part of the relative global attractor. Then we subdivide again and proceed in the same manner. Roughly speaking, we use *cell-mapping* techniques combined with a subdivision procedure to approach the global attractor (see e.g. [7, 8] for the description of cell-mapping). However, in contrast to the concept of cell-mapping, we are not interested in determining the full global dynamical behavior. Rather we use this concept to derive a numerical method which allows to approximate the global attractor up to a specified accuracy.

By construction, the algorithm provides in each step a covering of the relative global attractor under consideration. This covering becomes more and more accu-

rate — in the sense of decreasing Hausdorff distance to the global attractor — in the course of the iteration. Moreover, under the assumption that the relative global attractor has a hyperbolic structure and satisfies a shadowing property we can even obtain an asymptotic error estimate depending on the iteration step and the diameter of the boxes in that step. Essentially we show that from a certain subdivision step on the Hausdorff distance to the relative global attractor is less than or equal to twice the maximal diameter of the boxes in that step (cf. Proposition 4.10). This result is of particular interest since the "local methods" which are used for the computation of unstable manifolds do in general not allow to derive reasonable error estimates. The reason is that one has to expect sensitive dependence on initial conditions in the dynamical behavior close to unstable manifolds. We avoid this problem by approximating (global) unstable manifolds as *sets* (using a global approach) rather than as objects which consist of *single trajectories*.

In principle the application of the subdivision algorithm described in this article is not limited to systems in which the global attractor is low dimensional. Hence, this method can be used for the computation of higher dimensional unstable manifolds or global attractors as well. Indeed, we will illustrate this fact in §6 by the computation of two-dimensional unstable manifolds in three-dimensional dynamical systems. On the other hand, it is clear from the above description that the numerical effort depends on a combination of both the dimension of the underlying space and the dimension of the relative global attractor. For instance, the computation of a one-dimensional relative global attractor in an eight-dimensional space is an easy task in comparison to a four-dimensional relative global attractor in five-dimensional space. In the latter case an approximation may just be computed up to a very rough accuracy.

A more detailed outline of the paper is as follows. In §2 we recall some basic facts on attracting sets and we define the notion of relative global attractor. The subdivision algorithm is described in §3. In this section we also prove the convergence result mentioned above. In §4 we analyze the convergence behavior for the specific case where the relative global attractor has a hyperbolic structure. The implementation of the algorithm is discussed in §5, and, finally, in §6 we illustrate that the subdivision algorithm can successfully be applied by several numerical examples.

2 Attracting Sets and Relative Global Attractors

In this section we briefly recall some of the basic notions on invariant sets of dynamical systems. For a more detailed exposition the reader is e.g. referred to [3].

We consider discrete dynamical systems

$$x_{j+1} = f(x_j), \quad j = 0, 1, 2, \dots ,$$

where $f : \mathrm{R}^n \to \mathrm{R}^n$ is a diffeomorphism. Systems of this type arise, for instance, if one considers the time-one map or a Poincaré map of an ordinary differential equation. A subset $A \subset \mathrm{R}^n$ is called *invariant* if

$$f(A) = A.$$

Moreover, an invariant set A is an *attracting set* with *fundamental neighborhood* U if for every open set $V \supset A$ there is an $N \in \mathrm{N}$ such that $f^j(U) \subset V$ for all $j \geq N$. Observe that if A is invariant then the closure of A is invariant as well. Hence we may restrict our attention to closed invariant sets A, and in this case we obtain

$$A = \bigcap_{j \in \mathrm{N}} f^j(U).$$

By definition all the points in the fundamental neighborhood U are attracted by A. For this reason the open set $\cup_{j \in \mathrm{N}} f^{-j}(U)$ is called the *basin of attraction* of A. If the basin of attraction of A is the whole of R^n then A is called the *global attractor*.

Remark 2.1 (a) Observe that in general the global attractor may not be compact. However, in applications it can frequently be observed that all the orbits of the underlying dynamical system eventually lie inside a bounded domain in R^n, and in that case the compactness of A immediately follows.

(b) The global attractor contains all the invariant sets of the dynamical system. This can easily be verified using the definitions.

(c) At this point it should be emphasized that the global attractor is in general "invisible" in the sense that it cannot be computed by direct simulation of the underlying dynamical system. In fact, for this to be valid one would additionally need that A is *transitive*. However, the global attractor always contains all the subsets of R^n which can be approximated by direct simulation.

As already mentioned in the introduction the algorithm developed in this article can also be used to approximate global unstable manifolds. This claim is verified by showing that unstable manifolds are always contained in the global attractor if it is compact. We begin with the following definition.

DEFINITION 2.2 Let $x \in \mathrm{R}^n$. Then we call the sets

$$\begin{aligned} V^s(x) &= \{y \in \mathrm{R}^n : \lim_{j\to\infty} \|f^j(y) - f^j(x)\| = 0\} \\ V^u(x) &= \{y \in \mathrm{R}^n : \lim_{j\to-\infty} \|f^j(y) - f^j(x)\| = 0\} \end{aligned}$$

the *stable* and the *unstable set of* x respectively.

EXAMPLE 2.3 (a) Suppose that $p \in \mathrm{R}^n$ is a hyperbolic periodic point. Then $V^s(p) = W^s(p)$ and $V^u(p) = W^u(p)$ where $W^s(p)$ and $W^u(p)$ are the usual stable and unstable manifolds of p (see [11]).

(b) As a generalization of a hyperbolic periodic point one may consider a compact invariant set A with a hyperbolic structure (for a definition see §4). Also in this case the stable and unstable sets in Definition 2.2 coincide with the stable and unstable manifolds whose existence is shown in [6]. However, except for our convergence results in §4 we do not have to assume that the invariant set under consideration has a hyperbolic structure and hence it is more appropriate to introduce stable and unstable sets in this generality.

In terms of unstable manifolds instead of unstable sets the following result can be found in e.g. [3] (cf. Section III E).

PROPOSITION 2.4 *Let A be a compact attracting set. Then*

$$V^u(x) \subset A \text{ for all } x \in A.$$

The proof of this result is essentially the same as the corresponding result for unstable manifolds. However, we state its proof for the sake of completeness.
Proof: Let $x \in A$ and suppose that $y \in V^u(x)$. Let V be an open neighborhood of A and U a fundamental neighborhood. Since A is a compact attracting set there exists an $M \in \mathrm{N}$ such that $f^{-j}(y) \in U$ for all $j \geq M$. On the other hand there is an $N \in \mathrm{N}$ such that $f^j(U) \subset V$ for all $j \geq N$. Hence by taking $j \geq \max(M, N)$ we obtain

$$y = f^j(f^{-j}(y)) \in V.$$

Since V was arbitrary this completes the proof. □

In applications of our algorithm we approximate just a part of the global attractor within a specified compact set $Q \subset \mathrm{R}^n$. However, as we will see below, we do not approximate the entire part of the global attractor which is contained in Q. This motivates the following definition.

DEFINITION 2.5 Let $Q \subset \mathrm{R}^n$ be a compact set and let A be the global attractor. We define the *global attractor relative to* Q by

$$A_Q = \{x \in A \ : \ f^{-k}(x) \in Q \text{ for all } k \geq 0\} \ . \tag{2.1}$$

REMARK 2.6 (a) The definition of A_Q in (2.1) implies that $A_Q \subset Q$ and that $f^{-1}(A_Q) \subset A_Q$, but not necessarily that $f(A_Q) \subset A_Q$. In particular, A_Q may not be invariant. Observe that A_Q is compact since Q is compact, A is closed and f is a homeomorphism.

(b) Let A be the global attractor of f. Then in general

$$A_Q \neq A \cap Q.$$

To see this consider a heteroclinic connection between two hyperbolic fixed points p and q. Suppose that the unstable manifold of p is the stable manifold of q. Then we consider a compact set Q which contains q but not the entire heteroclinic connection to p (see Figure 1). Obviously the global attractor A contains the heteroclinic connection between p and q, but, on the other hand, the global attractor relative to Q does not contain the part of the heteroclinic connection between p and q which is inside Q. That is, A_Q is a proper subset of $A \cap Q$.

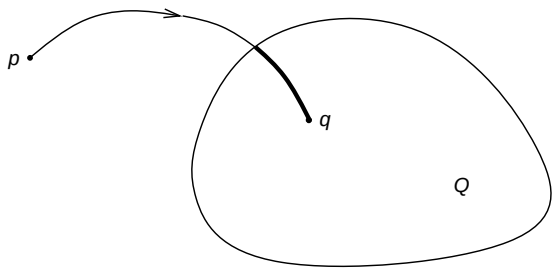

Figure 1: Illustration for the definition of a relative global attractor.

3 Approximation of Relative Global Attractors

In this section we describe the subdivision algorithm and we prove that it indeed allows to approximate relative global attractors.

Roughly speaking, the idea of the algorithm is as follows. We start with a finite family of (large) compact subsets of R^n which cover the domain in which we want to analyze the dynamical behavior. Then we subdivide each of these sets into

smaller ones and throw away subsets which do not contain part of the relative global attractor. Continuing the process with the new collection of (smaller) sets it becomes intuitively clear that this process should lead to a successively finer approximation of the relative global attractor.

Let us be more precise. The algorithm generates a sequence $\mathcal{B}_0, \mathcal{B}_1, \ldots$ of finite collections of compact subsets of R^n such that the diameter

$$\operatorname{diam}(\mathcal{B}_k) = \max_{B \in \mathcal{B}_k} \operatorname{diam}(B)$$

converges to zero for $k \to \infty$. Given an initial collection $\mathcal{B}_0$, we inductively obtain $\mathcal{B}_k$ from $\mathcal{B}_{k-1}$ for $k = 1, 2, \ldots$ in two steps.

1. *Subdivision:* Construct a new collection $\hat{\mathcal{B}}_k$ such that

$$\bigcup_{B \in \hat{\mathcal{B}}_k} B = \bigcup_{B \in \mathcal{B}_{k-1}} B \tag{3.1}$$

and

$$\operatorname{diam}(\hat{\mathcal{B}}_k) \leq \theta \operatorname{diam}(\mathcal{B}_{k-1}) \tag{3.2}$$

for some $0 < \theta < 1$.

2. *Selection:* Define the new collection $\mathcal{B}_k$ by

$$\mathcal{B}_k = \left\{ B \in \hat{\mathcal{B}}_k : \exists \hat{B} \in \hat{\mathcal{B}}_k \text{ such that } f^{-1}(B) \cap \hat{B} \neq \emptyset \right\} \tag{3.3}$$

The first step guarantees that the collections $\mathcal{B}_k$ consist of successively finer sets for increasing k. In fact, by construction

$$\operatorname{diam}(\mathcal{B}_k) \leq \theta^k \operatorname{diam}(\mathcal{B}_0) \to 0 \quad \text{for } k \to \infty.$$

In the second step we remove each subset whose preimage does neither intersect itself nor any other subset in $\hat{\mathcal{B}}_k$. As we shall see, this step is responsible for the fact that the unions $\bigcup_{B \in \mathcal{B}_k} B$ approach the relative global attractor.

EXAMPLE 3.1 Let us illustrate the algorithm for the simplest possible case, namely for the mapping $f : \mathrm{R} \to \mathrm{R}$,

$$f(x) = \alpha x,$$

with $\alpha \in (0, \frac{1}{2})$. With this choice of α the global attractor $A = \{0\}$ of f is a stable fixed point. We start with a single interval $\mathcal{B}_0 = \{[-1, 1]\}$ and construct $\hat{\mathcal{B}}_k$ by bisection of the intervals in $\mathcal{B}_{k-1}$. Hence,

$$\mathcal{B}_1 = \hat{\mathcal{B}}_1 = \{[-1, 0], [0, 1]\} \ .$$

No interval is removed, since each of them is mapped into itself. Subdividing again, we get four intervals

$$\hat{\mathcal{B}}_2 = \left\{[-1, -\frac{1}{2}], [-\frac{1}{2}, 0], [0, \frac{1}{2}], [\frac{1}{2}, 1]\right\} \ .$$

Applying the selection rule (3.3), the two boundary intervals are removed, i.e.

$$\mathcal{B}_2 = \left\{[-\frac{1}{2}, 0], [0, \frac{1}{2}]\right\} \ .$$

Proceeding this way, we obtain after k subdivision steps

$$\mathcal{B}_k = \left\{[-\frac{1}{2^{k-1}}, 0], [0, \frac{1}{2^{k-1}}]\right\} \ .$$

We see that the union $\bigcup_{B \in \mathcal{B}_k} B$ is indeed approaching the global attractor $A = \{0\}$ for $k \to \infty$. However, already this simple example shows that the convergence speed of the algorithm crucially depends on the contraction rate of the global attractor: if we would choose α to be between 0.5 and 1, then the stable fixed point would still be approached asymptotically but in a slower way. We will investigate this convergence behavior in detail in §4.

We now show that the algorithm described above always converges to a relative global attractor if k is going to infinity. Denote by Q_k the collection of compact subsets obtained after k subdivision steps, that is,

$$Q_k = \bigcup_{B \in \mathcal{B}_k} B.$$

We begin by noticing that the relative global attractor is always covered by these sets.

LEMMA 3.2 *Let A_Q be a global attractor relative to the compact set Q, and let $\mathcal{B}_0$ be a finite collection of closed subsets whose union is Q, i.e., $Q_0 = \bigcup_{B \in \mathcal{B}_0} B = Q$. Then the sets Q_k obtained by the subdivision algorithm contain the relative global attractor,*

$$A_Q \subset Q_k \quad \textit{for all } k \in \mathrm{N}.$$

Proof: By definition we know that $A_Q \subset Q = Q_0$. Suppose that there is an $x \in A_Q \subset Q_{k-1}$ such that $x \notin Q_k$ for some $k > 0$. Then there is a box $B \in \hat{\mathcal{B}}_k$ containing x which is removed in the selection step, i.e.

$$f^{-1}(B) \cap Q_{k-1} = \emptyset \ .$$

Hence, $f^{-1}(x) \notin Q_{k-1}$. But this contradicts the fact that $f^{-1}(A_Q) \subset A_Q \subset Q_{k-1}$ (see Remark 2.6(a)). ∎

The strategy for the proof of the main result is now as follows. Next we show that every subset of Q which is backward invariant must be contained in the relative global attractor. Then we prove that the limit of the Q_k's is indeed a backward invariant set and hence must be contained in A_Q. Finally, combining this with Lemma 3.2 gives the desired result.

LEMMA 3.3 *Let $B \subset Q$ be a subset such that*

$$f^{-1}(B) \subset B \ . \tag{3.4}$$

Then B is contained in the global attractor A_Q relative to Q.

Proof: By (3.4) we know that $B \subset f^k(B)$ for all $k \geq 0$. Therefore,

$$B \subset \bigcap_{k \geq 0} f^k(B) \subset \bigcap_{k \geq 0} f^k(U) = A \ ,$$

where A is the global attractor, and U its fundamental neighborhood. On the other hand, by (3.4) we also have that $f^{-k}(B) \subset B \subset Q$ for all $k \geq 0$. It follows that $B \subset A_Q$. ∎

Observe that the Q_k's define a nested sequence of compact sets, that is, $Q_{k+1} \subset Q_k$. Therefore, for each ℓ,

$$Q_l = \bigcap_{k=1}^{\ell} Q_k \ , \tag{3.5}$$

and we may view

$$Q_\infty = \bigcap_{k=1}^{\infty} Q_k$$

as the limit of the Q_k's.

LEMMA 3.4 *The set Q_∞ is a nonempty backward invariant set, i.e.,*

$$f^{-1}(Q_\infty) \subset Q_\infty \ .$$

Proof: First note that by Lemma 3.2, the limit set Q_∞ contains the relative global attractor A_Q. Therefore, in particular, Q_∞ is nonempty. We now show that Q_∞ is backward invariant. For contradiction suppose that there is a point $y \in Q_\infty$ such that $f^{-1}(y) \notin Q_\infty$. The fact that Q_∞ is compact implies that

$$d(f^{-1}(y), Q_\infty) > \delta > 0,$$

where d denotes the distance between $f^{-1}(y)$ and Q_∞. Hence there is an integer $N > 0$ such that

$$d\left(f^{-1}(y), Q_k\right) > \delta/2 \quad \text{for all } k > N$$

(see (3.5)). For each k choose a set $B_k(y) \in \mathcal{B}_k$ containing y. Then by continuity there is an $\ell > N$ such that

$$f^{-1}(B_\ell(y)) \cap Q_l = \emptyset.$$

But this is impossible by the construction of the algorithm, and we have obtained the desired contradiction. □

Now we are in the position to prove the following convergence result.

PROPOSITION 3.5 *Let A_Q be a global attractor relative to the closed set Q, and let $\mathcal{B}_0$ be a finite collection of closed subsets with $Q_0 = \bigcup_{B\in\mathcal{B}_0} B = Q$. Then*

$$A_Q = Q_\infty \, .$$

Proof: By Lemma 3.2 A_Q is contained in each Q_k and hence it is also contained in Q_∞. On the other hand, by Lemma 3.4 the compact set Q_∞ is backward invariant and thus Lemma 3.3 implies that it must be contained in the relative global attractor A_Q. In other words,

$$Q_\infty \subset A_Q \subset Q_\infty$$

which yields the desired result. □

REMARK 3.6 Recall that Q_∞ may be viewed as the limit of the Q_k's. Therefore the result of Proposition 3.5 can be restated as

$$\lim_{k\to\infty} h\left(A_Q, Q_k\right) = 0 \, ,$$

where we denote by $h(B, C)$ the usual Hausdorff distance between two compact subsets $B, C \subset \mathrm{R}^n$.

REMARK 3.7 We know from Proposition 2.4 that the global attractor A contains the union of the unstable sets of all the compact attracting sets of the dynamical system f. Hence, in particular, the above method allows us to construct approximations of *global* unstable manifolds. Moreover — as we will see in §4 — we can additionally control the error by means of the Hausdorff distance. We will illustrate this by examples in §6.

4 Convergence Behavior and Error Estimates

In this section we investigate the convergence behavior and we derive (local) error estimates for the subdivision algorithm described in the previous section. These results are obtained for the case where a hyperbolic structure is present. However, as will be illustrated by examples in §6, a similar convergence behavior can also be observed in more general situations.

We begin by recalling the definition of hyperbolic sets (see e.g. [15]).

DEFINITION 4.1 Let Λ be an invariant set for the diffeomorphism f. We say that Λ is a *hyperbolic set* for f if there is a continuous invariant splitting $T_\Lambda \mathrm{R}^n = E^s_\Lambda \oplus E^u_\Lambda$,

$$Df(E^s_x) = E^s_{f(x)} \quad \text{and} \quad Df(E^u_x) = E^u_{f(x)},$$

for which there are constants $c > 0$ and $\lambda \in (0,1)$, such that

a) if $v \in E^s_x$, then $\|Df^k(x)v\| \le c\lambda^k \|v\|$ for all $k \in \mathrm{N}$,

b) if $v \in E^u_x$, then $\|Df^{-k}(x)v\| \le c\lambda^k \|v\|$ for all $k \in \mathrm{N}$.

EXAMPLE 4.2 Let us consider the simplest example for a hyperbolic set, that is, the case where Λ is a hyperbolic fixed point p of f. Here E^s and E^u are the generalized eigenspaces corresponding to the eigenvalues of modulus less than or bigger than one respectively. Observe that there are no eigenvalues of modulus equal to one by the hyperbolicity of p.

Since the estimates in Definition 4.1 are formulated in terms of the Jacobians, they are just valid infinitesimally for f. The reader is probably familiar with the fact that hyperbolic fixed points also possess stable and unstable manifolds on which, roughly speaking, the same estimates hold for the diffeomorphism f itself. This fact — namely the existence of stable and unstable manifolds — holds generally for hyperbolic sets and this is essentially the contents of the Stable Manifold Theorem which we are now going to formulate. We begin by introducing the following notions.

DEFINITION 4.3 For $x \in \mathrm{R}^n$ and $\epsilon > 0$ we define the *local stable (unstable) manifold* by

$$\begin{aligned} W^s_\epsilon(x) &= \Big\{ y \in \mathrm{R}^n : d(f^k(x), f^k(y)) \to 0 \text{ for } k \to \infty \\ &\qquad \text{and } d(f^k(x), f^k(y)) \le \epsilon \text{ for all } k \ge 0 \Big\} , \\ W^u_\epsilon(x) &= \Big\{ y \in \mathrm{R}^n : d(f^k(x), f^k(y)) \to 0 \text{ for } k \to -\infty \\ &\qquad \text{and } d(f^k(x), f^k(y)) \le \epsilon \text{ for all } k \le 0 \Big\} . \end{aligned}$$

We now state part of the results which are known as the *Stable Manifold Theorem* for hyperbolic sets. A proof can be found in e.g. [15]. This theorem states in particular that the above defined sets $W^s_\epsilon(x)$ and $W^u_\epsilon(x)$ are for small ϵ indeed smooth manifolds, and this justifies the terms local stable and local unstable manifold.

THEOREM 4.4 *Let Λ be a closed hyperbolic set for f. Then there is a positive ϵ such that for every point $x \in \Lambda$, $W^s_\epsilon(x)$ and $W^u_\epsilon(x)$ are embedded disks of dimension equal to those of E^s_x and E^u_x respectively. The tangent space of $W^s_\epsilon(x)$ ($W^u_\epsilon(x)$) at x is E^s_x (E^u_x).*

Moreover, $W^s_\epsilon(x)$ and $W^u_\epsilon(x)$ satisfy the following properties:

1. *There is a constant $C > 0$ such that*

$$\begin{aligned} d(f^k(x), f^k(y)) &\le C\lambda^k d(x,y), \quad \textit{for all } y \in W^s_\epsilon(x) \textit{ and } k \ge 0, \\ d(f^{-k}(x), f^{-k}(y)) &\le C\lambda^k d(x,y), \quad \textit{for all } y \in W^u_\epsilon(x) \textit{ and } k \ge 0, \end{aligned}$$

   where λ is chosen according to Definition 4.1.

2. *The local stable and unstable manifolds are given by*

$$\begin{aligned} W^s_\epsilon(x) &= \Big\{ y \in \mathrm{R}^n : d(f^k(x), f^k(y)) \le \epsilon \textit{ for all } k \ge 0 \Big\} , \\ W^u_\epsilon(x) &= \Big\{ y \in \mathrm{R}^n : d(f^k(x), f^k(y)) \le \epsilon \textit{ for all } k \le 0 \Big\} . \end{aligned}$$

We may use Theorem 4.4 to obtain a result on the convergence behavior of our subdivision algorithm in the case where the relative global attractor is part of a compact hyperbolic set which possesses the *shadowing property*.

DEFINITION 4.5 Let $\delta > 0$. Then a sequence of points $x_k \in \mathrm{R}^n$, $k \in \mathrm{Z}$, is a *δ-pseudoorbit* if $|f(x_k) - x_{k+1}| < \delta$ for all $k \in \mathrm{Z}$. Given $\epsilon > 0$, $x \in \Lambda$ is an *ϵ-tracing point in* Λ for a pseudoorbit $\{x_k\}$ if $|f^k(x) - x_k| < \epsilon$ for all $k \in \mathrm{Z}$.

DEFINITION 4.6 The set Λ has the *shadowing property* if for every $\epsilon > 0$ there is a $\delta > 0$ such that every δ-pseudoorbit in Λ has an ϵ-tracing point.

REMARK 4.7 We remark that for a hyperbolic set Λ the shadowing property is equivalent to the existence of a *local product structure* and also to the fact that periodic points are dense in Λ (see [15]).

The following result is due to [5]. A proof can be found in e.g. [15, 1].

PROPOSITION 4.8 *Suppose that Λ is a compact hyperbolic set which satisfies the shadowing property, and let $\tilde{\epsilon}$ be a positive constant less than $\epsilon/2$, where ϵ is chosen according to Theorem 4.4.*

Then there is a constant δ and a neighborhood U of Λ such that every δ-pseudoorbit in U is $\tilde{\epsilon}$ shadowed by a point y in Λ. In particular, every point in U is contained in a stable manifold of a point of Λ.

After these preliminary considerations we are now in the position to state the main result of this section. To simplify the statement we formulate it for a power of f rather than for f itself. More precisely, using the notation of Theorem 4.4 we choose $q \in \mathrm{N}$ in such a way that

$$C\lambda^q < \frac{1}{2}$$

and define a new diffeomorphism g by

$$g = f^q = \underbrace{f \circ \cdots \circ f}_{q \text{ times}}.$$

REMARK 4.9 (a) Note that the relative global attractors of f and f^q, $q \geq 2$, are in general not identical. (To construct such an example choose Q to be a neighborhood of one element of a period two orbit and set $g = f^2$.) However, it can easily be seen that the global attractors of f and f^q are identical for each power q, and with this observation it follows directly from the definition that each relative global attractor of f is a relative global attractor of f^q as well. In this sense no information on the dynamical behavior is lost if we consider a power of f rather than the diffeomorphism f itself.

(b) We also remark that if the global attractor of f consists of the union of invariant sets which are *topologically mixing* then the relative global attractors of f and f^q are the same. This follows from the fact that topologically mixing invariant sets are transitive sets for f^q for each power of q (see [9]).

PROPOSITION 4.10 *Let A_Q be a global attractor of the diffeomorphism g relative to the closed set Q, and suppose that A_Q is contained in a compact hyperbolic set which satisfies the shadowing property. Then there is an integer N such that for each subdivision step $k \geq N$ performed with g the following error estimate holds:*

$$h(A_Q, Q_k) \leq 2\,\mathrm{diam}(\mathcal{B}_k). \tag{4.1}$$

Proof: Let U be the neighborhood of the closed hyperbolic set containing A_Q which is chosen according to Proposition 4.8. Let $\rho = h(\overline{U \cap Q}, A_Q)$. By Proposition 3.5 we know that the Q_k's converge to A_Q and hence we can find an N such that

$$h(A_Q, Q_k) < \frac{\rho}{2}$$

for all $k \geq N$.

For contradiction we assume that there is an $\ell > N$ such that

$$h(A_Q, Q_\ell) = 2\,\mathrm{diam}(\mathcal{B}_\ell) + \delta$$

with $\delta > 0$. Then there is a closed subset $B_0 \in \mathcal{B}_\ell$ such that all points in B_0 have at least distance $\mathrm{diam}(\mathcal{B}_\ell) + \delta$ to the relative global attractor A_Q. In particular, B_0 cannot have a nonempty intersection with any of the unstable manifolds since those are contained in A_Q (use Proposition 2.4 and the definition of relative global attractors). Proposition 4.8 now guarantees that B_0 is entirely contained in the union of the local stable manifolds and by the choice of q and N it follows that all points in the preimage of B_0 have at least a distance $2(\mathrm{diam}(\mathcal{B}_\ell) + \delta)$ to A_Q. In particular, $f^{-1}(B_0) \cap B_0 = \emptyset$.

By the construction of the subdivision algorithm it follows that there is another closed set $B_1 \in \mathcal{B}_\ell$ such that $f^{-1}(B_0) \cap B_1 \neq \emptyset$. Now all the points in B_1 have at least distance $\mathrm{diam}(\mathcal{B}_\ell) + 2\delta$ to the relative global attractor A_Q and we may use the same argument as for B_0 to conclude that $f^{-1}(B_1) \cap B_1 = \emptyset$. Hence there is a closed subset $B_2 \in \mathcal{B}_\ell$ such that $f^{-1}(B_1) \cap B_2 \neq \emptyset$ and all the points in B_2 have at least distance $\mathrm{diam}(\mathcal{B}_\ell) + 4\delta$ to the relative global attractor A_Q.

Proceeding inductively we construct a sequence $\{B_j\}$ of elements of $\mathcal{B}_\ell$ such that eventually the distance $h(A_Q, B_j)$ will be greater than $\rho/2$. But this is impossible by the choice of N and establishes the desired contradiction. □

With the following example we illustrate the convergence result of Proposition 4.10. It follows from this example that the error estimate (4.1) is sharp.

EXAMPLE 4.11 Let us go back to Example 3.1 and consider the mapping

$$f(x) = \alpha x,$$

with $\alpha = 0.5 - \epsilon$ and $0 < \epsilon < 0.01$. We start with the interval

$$\mathcal{B}_0 = \{[-1 + 10\epsilon, 1 + 10\epsilon]\}$$

and construct $\hat{\mathcal{B}}_k$ by bisection of the intervals in $\mathcal{B}_{k-1}$. Hence,

$$\mathcal{B}_1 = \hat{\mathcal{B}}_1 = \{[-1 + 10\epsilon, 10\epsilon], [10\epsilon, 1 + 10\epsilon]\} .$$

No interval is removed, since the image of each of them under f has a nonzero intersection with itself. Subdividing again, we get four intervals

$$\hat{\mathcal{B}}_2 = \{[-1 + 10\epsilon, -0.5 + 10\epsilon], [-0.5 + 10\epsilon, 10\epsilon], [10\epsilon, 0.5 + 10\epsilon], [0.5 + 10\epsilon, 1 + 10\epsilon]\} .$$

Applying the selection rule (3.3), just the interval $[0.5 + 10\epsilon, 1 + 10\epsilon]$ is removed since $f(-1 + 10\epsilon) \in [-1 + 10\epsilon, -0.5 + 10\epsilon]$. Therefore

$$\mathcal{B}_2 = \{[-1 + 10\epsilon, -0.5 + 10\epsilon], [-0.5 + 10\epsilon, 10\epsilon], [10\epsilon, 0.5 + 10\epsilon]\} .$$

In particular we see that $h(0, Q_2) = 1 - 10\epsilon < 1 = 2\,\mathrm{diam}(\mathcal{B}_2)$, and it follows that we may get arbitrarily close to $2\,\mathrm{diam}(\mathcal{B}_2)$ by shrinking ϵ. This shows that the estimate in Proposition 4.10 is optimal.

5 Implementation of the Subdivision Algorithm

In this section we describe the details concerning the implementation of the algorithm, and we discuss the computational effort that is needed. To make the description more transparent we break it up into several subsections.

Realization of the Subdivision Step

We realize the closed subsets constituting the collections $\mathcal{B}_k$ using generalized rectangles of the form

$$R(c, r) = \{y \in \mathrm{R}^n : |y_i - c_i| \le r_i \text{ for } i = 1, \dots, n\} \ ,$$

where $c, r \in \mathrm{R}^n$, $r_i > 0$ for $i = 1, \dots, n$, are the center and the radius respectively. We start the subdivision algorithm with a single rectangle $\mathcal{B}_0 = \{R\}$. In the k-th subdivision step we subdivide each rectangle $R(c, r) \in \mathcal{B}_k$ of the current collection by bisection with respect to the j-th coordinate, where j is varied cyclically, that

is, $j = ((k-1) \mod n) + 1$. This division leads to two rectangles $R_-(c^-, \hat{r})$ and $R_+(c^+, \hat{r})$, where

$$\hat{r}_i = \begin{cases} r_i & \text{for } i \neq j \\ r_i/2 & \text{for } i = j \end{cases}, \quad c_i^{\pm} = \begin{cases} c_i & \text{for } i \neq j \\ c_i \pm r_i/2 & \text{for } i = j \end{cases}.$$

We perform the subdivision until a prescribed size ϵ of the diameter relative to the initial rectangle is reached. That is, we stop when

$$\operatorname{diam}(\mathcal{B}_k) < \epsilon \operatorname{diam}(Q).$$

By definition, ϵ is a measure for the accuracy of the approximation.

Realization of the Selection Step

For the selection step (3.3), we have to decide whether or not the preimage of a given set $B_i \in \mathcal{B}_k$ has a nonzero intersection with another set $B_j \in \mathcal{B}_k$, i.e.

$$f^{-1}(B_i) \cap B_j = \emptyset \, ? \tag{5.1}$$

In simple model problems such as our trivial Example 3.1 this decision can be made analytically. For more complex problems we have to use some kind of *discretization*. Motivated by similar approaches in the context of cell-mapping techniques (see [7]), we choose a finite set of test points in each set $B_j \in \mathcal{B}_k$ and replace the condition (5.1) by

$$f(x) \notin B_i \text{ for all test points } x \in B_j \, . \tag{5.2}$$

Obviously, it may still occur that $f^{-1}(B_i) \cap B_j$ is nonempty although (5.2) is valid. To make the algorithm more robust, we therefore reintroduce rectangles if an image $f(x)$ of a test point x is not contained in any set B_j of the current collection. By this additional feature we make sure that the union of the B_j's are at each step of the algorithm a good approximation of a covering of the relative global attractor.

It remains to discuss how the test points are distributed inside each rectangle. To define the test points, observe that $R(c, r)$ is the affine image of the standard cube $[-1, 1]^n$ scaled by r and translated by c. Using this transformation it is sufficient to define the test points for the standard cube. Simple geometric considerations make it clear that one should obtain the best results for the test in (5.2) if most of the test points are lying on the boundary of the rectangle. In the present implementation, we use N test points on each edge distributed according to

$$t(\ell) = \frac{2\ell - 1}{N} - 1 \text{ for } \ell = 1, ..., N \tag{5.3}$$

on $[-1,1]$. As an additional test point we choose the center $c = 0$. Hence, in n-dimensional problems we have $p = n2^{n-1}$ test points per rectangle.

REMARK 5.1 For higher space dimension, say $n \geq 8$, a stochastic choice of the test points appears to be more appropriate. These questions will be explored in more detail in a forthcoming paper where also the computation of invariant measures is considered. However, for the present purposes the choice according to (5.3) turned out to be perfectly adequate.

Storage of the $\mathcal{B}_k$'s

The collections $\mathcal{B}_k$ can easily be stored in a binary tree. In Figure 2 we show the representation of three subdivision steps in two dimensions ($n = 2$) together with the corresponding sets Q_k, $k = 0, 1, 2, 3$. Note that each $\mathcal{B}_k$ and the corresponding covering Q_k are completely determined by the tree structure, and the initial box $R(c, r)$. Using this scheme, the memory requirements grow only linear in the dimension n of the problem.

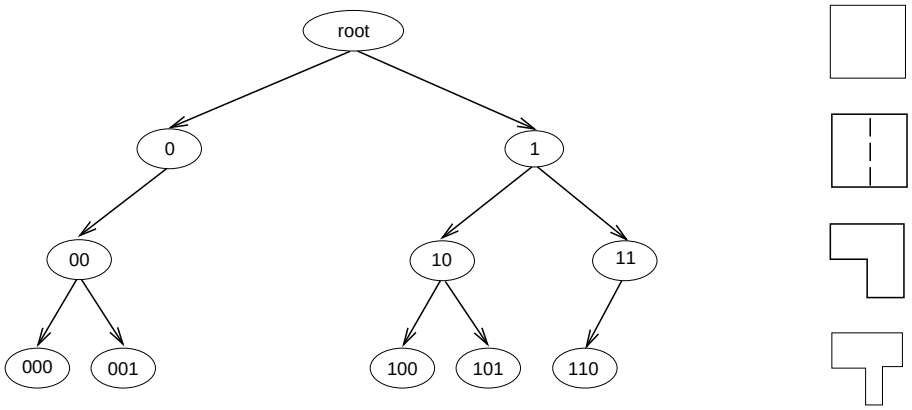

Figure 2: Storage scheme for the collections $\mathcal{B}_k$, $k = 0, 1, 2, 3$.

Amount of Work

We restrict our discussion to the implementation on a serial computer. Obviously, the inherent hierarchical structure of the algorithm makes it easy to break the com-

putational task into large pieces which can be performed in parallel (*coarse grain parallelism*).

There are two possibilities to implement the subdivision algorithm: either we minimize the floating point operations, or we try to be as memory efficient as possible. In the first case we have to keep the characterizing quantities, namely the center $c \in \mathrm{R}^n$ and the radius $r \in \mathrm{R}^n$, for each box. Since the number of boxes is usually quite large, this strategy would soon exceed the fast memory and thus slow down the computation, even for moderate dimensions n. Since we aim at high dimensional problems, this approach appears prohibitive.

Minimizing the memory requirements means to store nothing but the initial box $R(c, r)$ and the tree structure as described in the previous subsection. We then have to recalculate the center and radius of a particular box whenever it is used. Of course, we organize the algorithm in a hierarchical (recursive) manner avoiding unnecessary computations of the same quantities c and r. Moreover, observe that these calculations usually contribute only a minor part to the total cost. In fact, in most applications the computational work is dominated by the evaluations of the right hand side f of the dynamical system, being defined as a complicated nonlinear function or even as a time discretization of the flow of an ordinary differential equation ("time T map").

To determine the computational effort let us consider the k-th subdivision step, that is, the computation of $\mathcal{B}_k$ from $\mathcal{B}_{k-1}$. Let N_ℓ denote the number of boxes in the collection $\mathcal{B}_\ell$, and let p be the number of test points in each box. Constructing the next collection by bisection, we obtain $2N_{k-1}$ elements in $\hat{\mathcal{B}}_k$. Thus, we have to map

$$F_k = 2pN_{k-1}$$

test points x and look for the corresponding boxes $B \in \hat{\mathcal{B}}_k$ containing $f(x)$. This search is most easily realized as a binary search in the tree structure representing $\hat{\mathcal{B}}_k$. Including the computation of the centers and radii, each search involves $3k$ flops. The effort to compute the actual test points is $O(F_k)$ and may usually be neglected in comparison to the same number of f-evaluations. Hence, we end up with

a) $F_k = 2pN_{k-1}$ function evaluations, and

b) $3kF_k = 6kpN_{k-1}$ flops for the binary search.

We see that for small k the mapping of the test points is the most time consuming part of the calculations. When an f evaluation becomes less expensive than $3k$ flops, then the binary search is going to dominate.

REMARK 5.2 Observe that a non-neglectable portion of the computational effort is spent on the dynamical memory allocation. This part is not easy to quantify, because it also strongly depends on the actual platform used. Note, however, that due to the simple structure of the binary tree, it is fairly easy to optimize this part of the algorithm. For instance, the nodes of the tree are of fixed size, and the number of boxes constructed in the next iteration step is known in advance, allowing an adapted memory allocation.

6 Numerical Examples

EXAMPLE 6.1 We begin by considering a two dimensional dynamical system, the (scaled) Henon map

$$f(x) = \begin{pmatrix} 1 - ax_1^2 + x_2/5 \\ 5bx_1 \end{pmatrix}. \tag{6.1}$$

In our computations we have set $b = 0.2$ and $a = 1.2$. Starting with the square $[-2, 2]^2$, we display in Figure 3 the coverings obtained by the algorithm after $k = 6, 8, 10, 12$ subdivision steps corresponding to the relative accuracies $\epsilon = 2^{-k/2}$. We have used $N = 3$ test points per edge yielding $p = 13$ test points for each box. We can see that after 12 subdivision steps we already have a very good idea about the structure of the relative global attractor. However, in Figure 4(a) we show the rectangles covering the relative global attractor after 18 subdivision steps. After this number of steps the diameter of the boxes is already 0.011, but the computation just takes about 8 cpu seconds on a SUN SPARCstation 20.

We remark that a direct simulation would not yield the same result. In Figure 4(b) we illustrate this fact by showing the attractor that appears if the transient behavior has been neglected. The reason for the difference lies in the fact that the subdivision algorithm approximates all the unstable manifolds of hyperbolic sets in $[-2, 2]^2$. In particular, the one-dimensional unstable manifolds of the two hyperbolic fixed points (marked with circles in Figure 4(b)) are approximated — but those cannot be computed by direct simulation.

Finally, we illustrate the validity of our convergence result by the consideration of the hyperbolic fixed point at $(-1.3052, -1.3052)$. The contraction rate along its stable manifold is approximately $0.0626 < 0.5$, and therefore we may apply Proposition 4.10 to a neighborhood of this fixed point with $g = f$. We show part of the covering of the unstable manifold after 18 subdivision steps in Figure 5. As expected for this large number of steps it can be observed that the Hausdorff distance of $\mathcal{B}_{18}$ to the unstable manifold is indeed less than twice the diameter of $\mathcal{B}_{18}$.

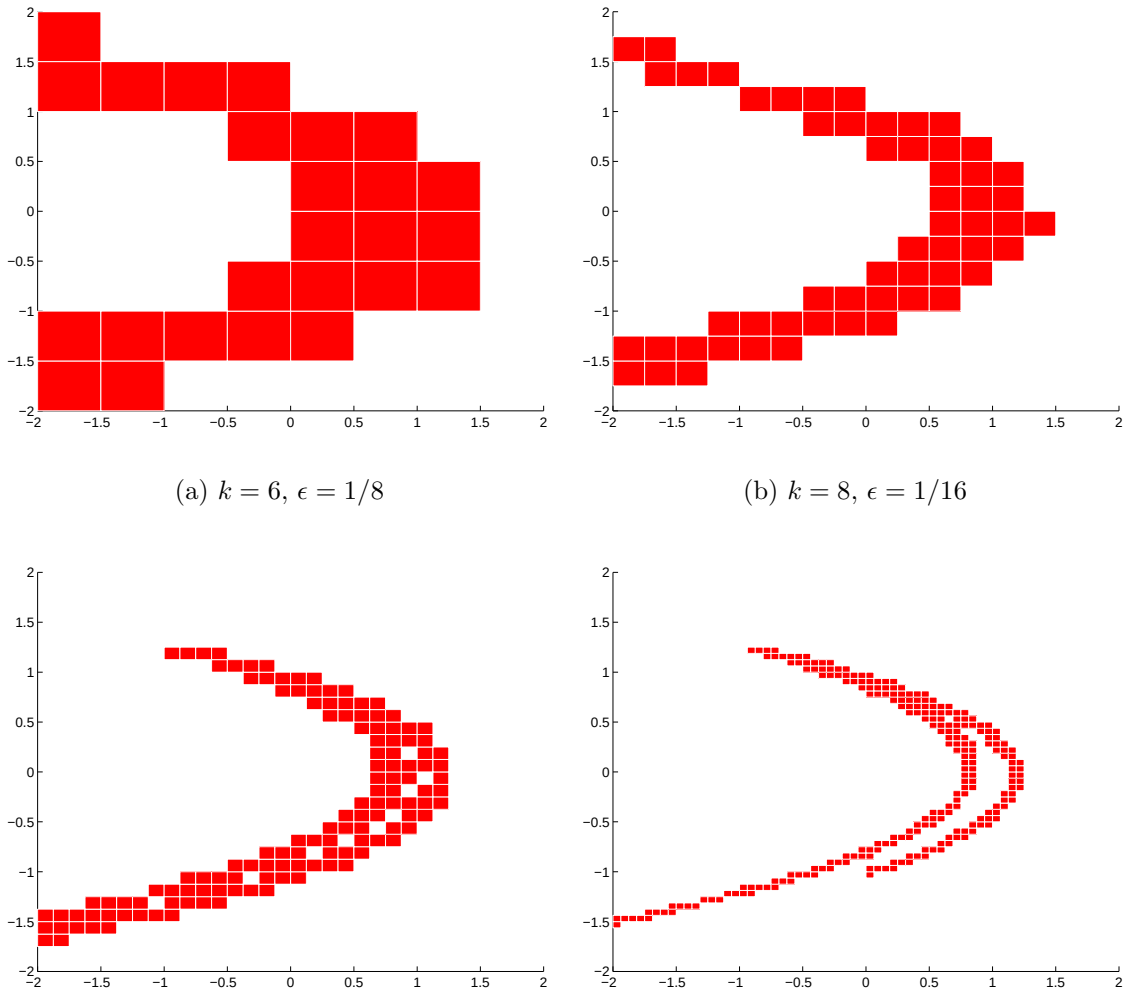

(a) $k = 6$, $\epsilon = 1/8$

(b) $k = 8$, $\epsilon = 1/16$

(c) $k = 10$, $\epsilon = 1/32$

(d) $k = 12$, $\epsilon = 1/64$

Figure 3: Successively finer coverings of the global Henon attractor.

EXAMPLE 6.2 In this example we illustrate the fact that the subdivision algorithm is particularly useful for the approximation of attractors in the case where — on average — it takes a long time by direct simulation to encouter certain parts of it.

Again we consider the Henon mapping f in (6.1). This diffeomorphism maps the two parts of the attractor shown in Figure 4(b) onto each other, and therefore each half is an invariant set for $f^2 = f \circ f$. Moreover, these invariant sets approach the upper right fixed point and eventually collide at it if the parameter a is increased up to $a \approx 1.27061312$ while $b = 0.2$ is kept fixed (see [2]). Right after the collision it

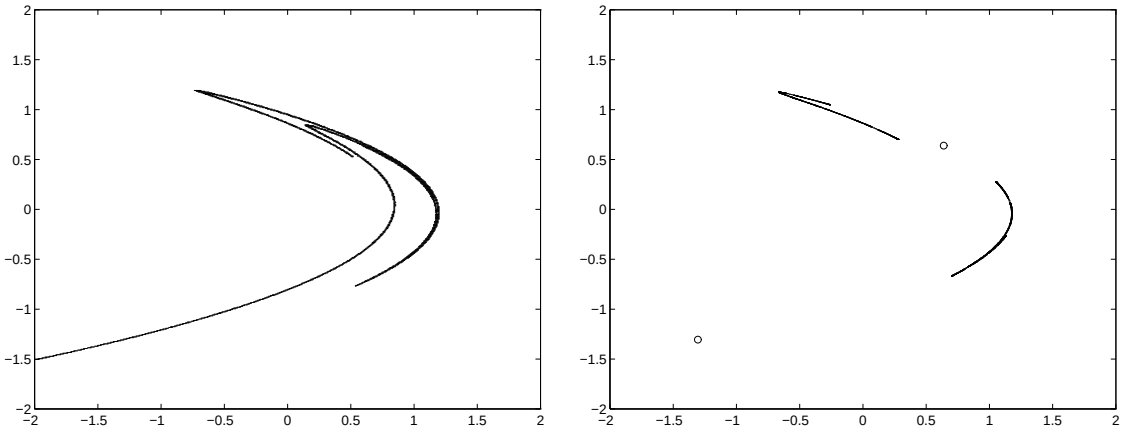

(a) Subdivision (b) Simulation

Figure 4: (a) Approximation of the relative global attractor for the Henon mapping after 18 subdivision steps ($\epsilon \approx 1.95 \cdot 10^{-3}$); (b) attractor of the Henon mapping computed by direct simulation. The two hyperbolic fixed points are marked with $\circ$.

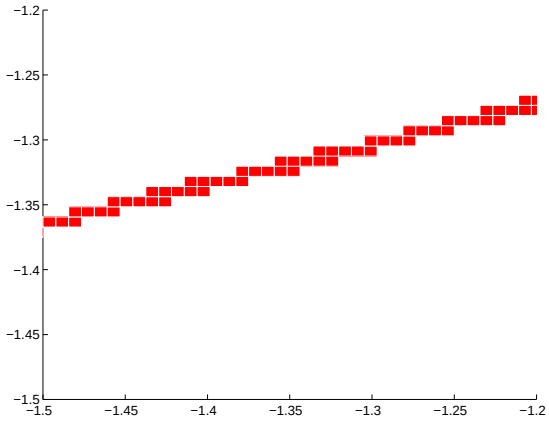

Figure 5: Magnification of part of the approximation in Figure 4(a).

takes quite a long time for single trajectories on the attractor to change from "one side to the other". Indeed, in Figure 6(b) we show the result of a direct simulation of f^2 for $a = 1.27061315$ where we have used 20000 iterates. In contrast to this result we display in Figure 6(a) the approximation by the subdivision algorithm after 18 steps starting with the rectangle $Q = [-1, 1.5]^2$. By construction, the subdivision algorithm approximates the full attractor and not just part of it. In other words, the

algorithm is not influenced by the fact that single orbits visit different parts of the attractor in a nonuniform way. This again confirms the advantage of our approach in which we aim for the approximation of *sets* rather than the approximation of *single orbits*.

Finally observe that in Figure 6(a) we do not cover part of the unstable manifold of the fixed point at $(-1.3052, -1.3052)$ as in Figure 4(a). The reason is that the algorithm approximates the global attractor relative to $Q = [-1, 1.5]^2$ and this box does no longer contain this fixed point any more. Hence its unstable manifold is not part of the relative global attractor and we have encountered a situation which is very similar to that in Figure 1.

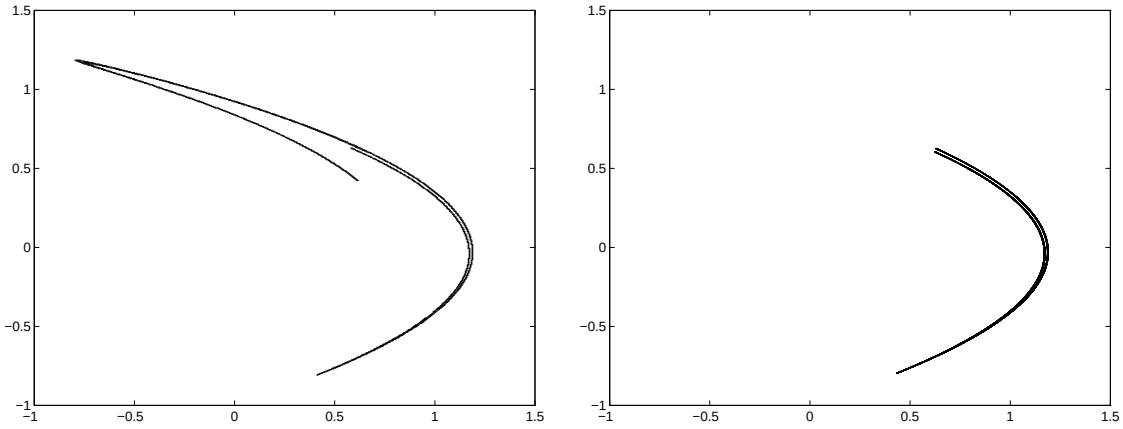

(a) Subdivision (b) Simulation

Figure 6: (a) Approximation of the relative global attractor of f^2 after 18 subdivision steps ($a = 1.27061315$); (b) part of the attractor of f^2 computed by direct simulation using 20000 iterates.

EXAMPLE 6.3 As the first three dimensional example, we consider the following map

$$f(x) = \begin{pmatrix} x_2 - \mu x_1 \\ \lambda x_2(1 - x_1) \\ x_1 - \gamma x_3 \end{pmatrix}. \tag{6.2}$$

We set $\lambda = 2.35$, $\mu = 0.5$, and $\gamma = 0.1$. As the starting rectangle for our subdivision algorithm we have chosen

$$[-0.38, 0.98] \times [0.05, 1.45] \times [-0.38, 0.98].$$

In Figure 7 we show the coverings obtained after $k = 5, 8, 11, 14$ subdivision steps. We remark that in this case the (fractal) dimension of the relative global attrac-

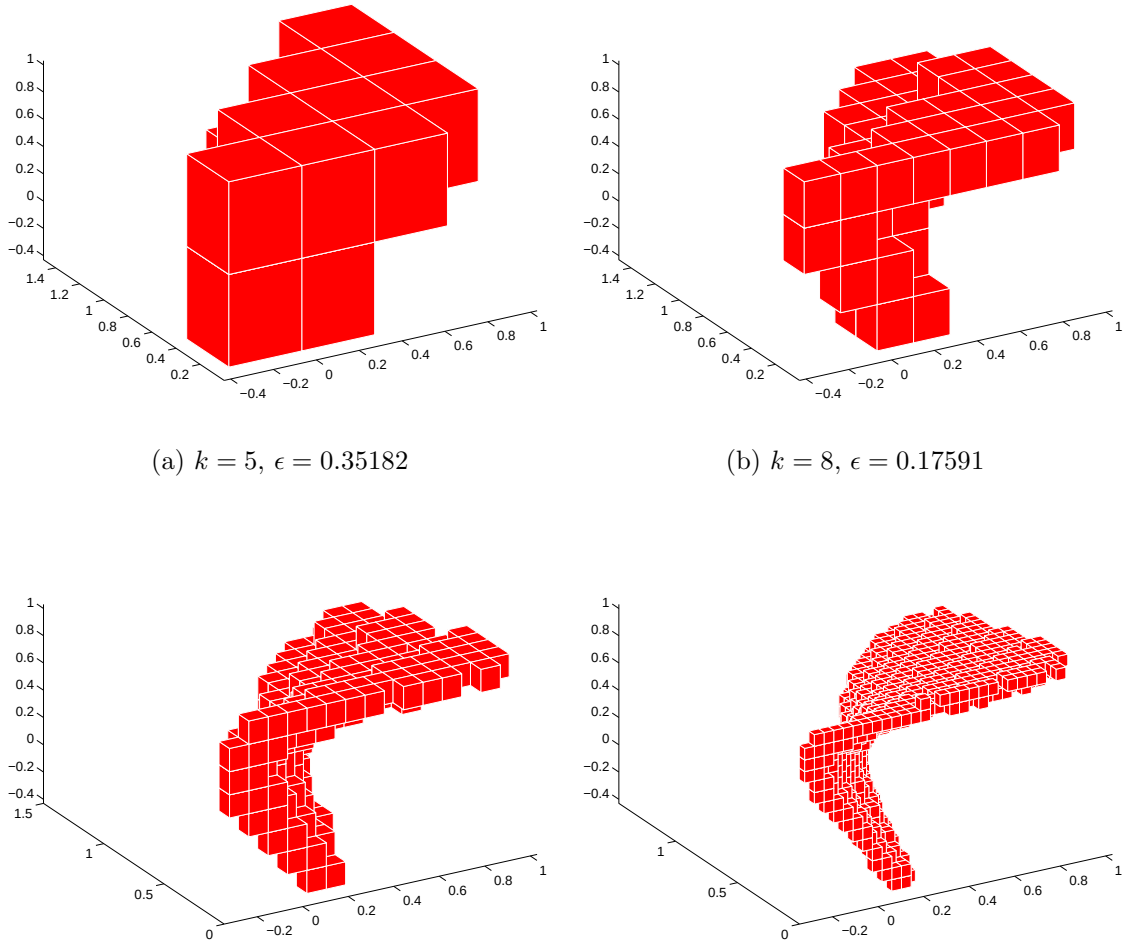

(a) $k = 5$, $\epsilon = 0.35182$

(b) $k = 8$, $\epsilon = 0.17591$

(c) $k = 11$, $\epsilon = 0.08796$

(d) $k = 14$, $\epsilon = 0.04398$

Figure 7: Successively finer coverings of a relative global attractor for (6.2) together with corresponding accuracies.

tor is greater or equal to two. Indeed, it is easy to see that for our choice of the parameter values the mapping (6.2) has a hyperbolic fixed point at $(x_1, x_2, x_3) = (0.5745, 0.8617, 0.5222)$ with a two-dimensional unstable manifold. Hence our computations suggest that we have approximated the global unstable manifold of that fixed point.

In Figure 8 we show the midpoints of the rectangles covering the attractor after 22 subdivision steps. Finally we remark that by direct simulation of (6.2) with an

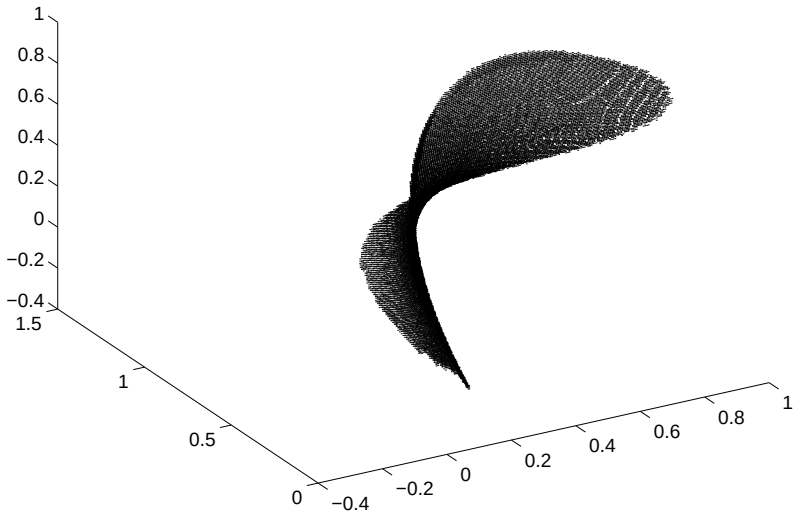

Figure 8: Approximation of the relative global attractor for (6.2) after 22 subdivsion steps ($\epsilon = 0.00679$).

initial value with positive components one just obtains a periodic point of period six once the transient behavior has been neglected. Similar to Example 6.1 this periodic point is a proper subset of the relative global attractor shown in Figure 8.

Example 6.4 As the last example we consider the three dimensional first order ordinary differential equation known as *Chua's circuit*,

$$\begin{aligned} \dot{x} &= \alpha(y - m_0 x - \frac{1}{3} m_1 x^3) \\ \dot{y} &= x - y + z \\ \dot{z} &= -\beta y \end{aligned}$$

where we have chosen $\alpha = 18$, $\beta = 33$, $m_0 = -0.2$ and $m_1 = 0.01$. These equations describe the dynamical behavior of an autonomous electrical circuit. Concerning the technical details of this model the reader is referred to e.g. [10].

We consider the diffeomorphism f given by the corresponding time-one map, and we analyze the dynamical behavior in $Q = [-12, 12] \times [-2.5, 2.5] \times [-20, 20]$. The results of the subdivision algorithm for $k = 8, 11, 20$ steps are displayed in Figure 9.

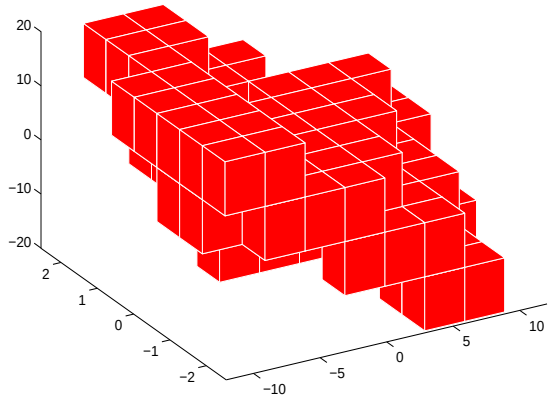

(a) $k = 8$, $\epsilon = 0.22294$

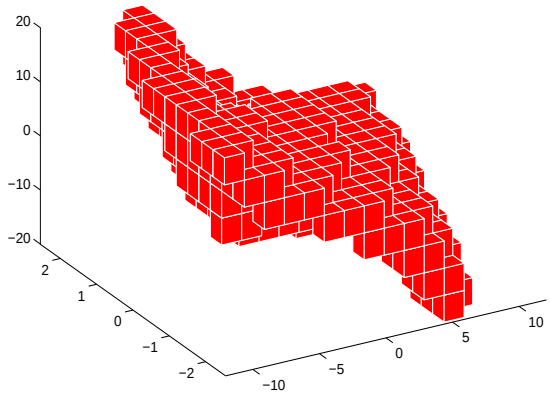

(b) $k = 11$, $\epsilon = 0.11147$

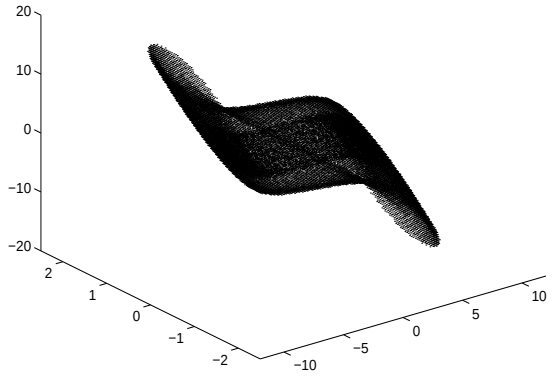

(c) $k = 20$, $\epsilon = 0.013934$

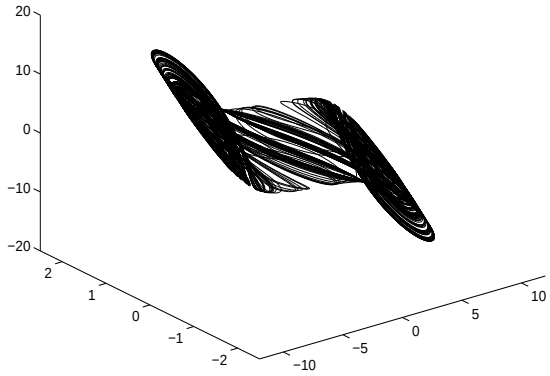

(d) Simulation

Figure 9: (a)-(c) Successively finer coverings of a relative global attractor for Chua's circuit together with corresponding accuracies; (d) approximation obtained by direct simulation.

In this figure we also show an approximation of the attractor obtained by direct simulation. With each of these computations we have approximated the union of the global unstable manifolds of the three steady state solutions contained in Q. (It is an elementary computation to show that the right hand side in Chua's circuit has precisely three zeros in Q.) Two of those equilibria have unstable manifolds of

dimension two and therefore the fractal dimension of the relative global attractor is greater or equal to two. We remark that just two test points per edge were needed in all the computations (see (5.2), (5.3)).

Finally we demonstrate in Figure 10 that the approximation by the subdivision algorithm does not possess any holes in contrast to the approximation of the attractor obtained by direct simulation. Since there is numerical evidence that all the steady states in Q are part of the attractor we may conclude that this attractor contains the related global unstable manifolds as well (see Proposition 2.4). Since these are automatically covered by the relative global attractor, our approximation by the subdivision algorithm is more precise than the one obtained by direct simulation. However, if we additionally assume that the attractor is transitive, then the holes would be filled by a typical trajectory as well; but this may take a very long time of integration.

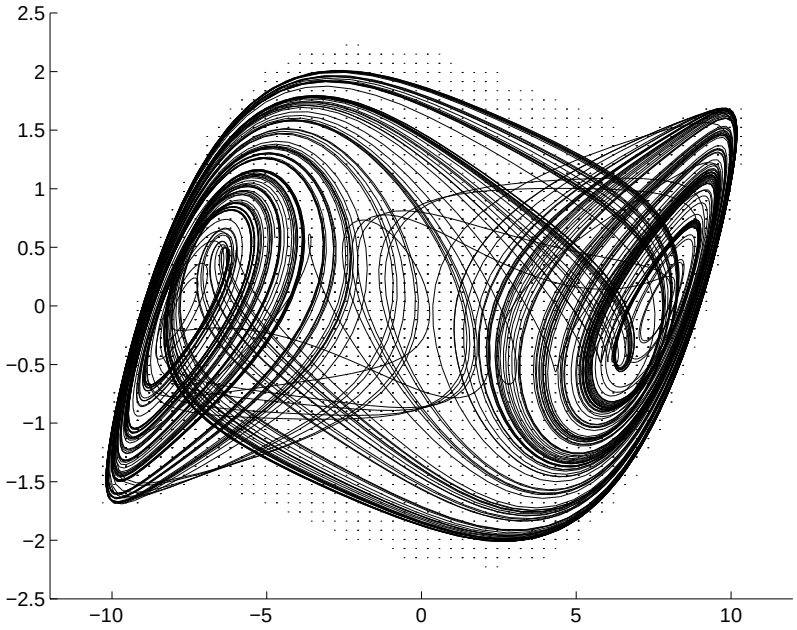

Figure 10: The dots represent the centers of boxes of an approximation of the relative global attractor obtained after 18 subdivsion steps. Superimposed is a trajectory computed by direct simulation. We show a projection onto the (x, y)-plane.

Acknowledgments We are grateful Ian Melbourne for very helpful discussions. Both authors acknowledge the hospitality of the Department of Mathematics at the University of Houston where this work has been carried out.

References

[1] R. Bowen. *Equilibrium States and the Ergodic Theory of Axiom A Diffeomorphisms*, Lecture Notes in Mathematics **470**, (Springer, 1975).

[2] M. Dellnitz. Symmetry creation via collisions of attractors, Habilitation thesis, Hamburg, 1994.

[3] J.-P. Eckmann and D. Ruelle. Ergodic theory of chaos and strange attractors, *Reviews of Modern Physics*, **57** (3) I (1985), 617-656.

[4] J. Guckenheimer and P. Holmes. *Nonlinear Oscillations, Dynamical Systems, and Bifurcations of Vector Fields*, (Springer, 1986).

[5] M.W. Hirsch, J. Palis, C.C. Pugh and M. Shub. Neighborhoods of hyperbolic sets, *Invent. Math.*, **9** (1969-70), 121.

[6] M.W. Hirsch and C.C. Pugh. Stable manifolds and hyperbolic sets, *Proc. Symp. Pure Math.*, **14** (1970), 133-163.

[7] C.S. Hsu. Global analysis by cell mapping, *Int. J. Bif. Chaos*, **2** (4) (1992), 727-771.

[8] E. Kreuzer. *Numerische Untersuchung Nichtlinearer Dynamischer Systeme*, (Springer, 1987).

[9] R. Mañé. *Ergodic Theory and Differentiable Dynamics*, (Springer, 1987).

[10] T. Matsumoto, L. O. Chua and M. Komuro. The double scroll, *IEEE Transactions on Circuits and Systems*, **32**(8) (1985), 797-818.

[11] J. Palis and W. de Melo. *Geometric Theory of Dynamical Systems*, (Springer, 1982).

[12] J. Palis and F. Takens. *Hyperbolicity & Sensitive Chaotic Dynamics at Homoclinic Bifurcations*, (Cambridge University Press, 1993).

[13] T.S. Parker and L.O. Chua. *Practical Numerical Algorithms for Chaotic Systems*, Springer, New York, (1989).

[14] D. Ruelle. Small random perturbations of dynamical systems and the definition of attractors, *Commun. Math. Phys.*, **82** (1981), 137-151.

[15] M. Shub. *Global Stability of Dynamical Systems*, (Springer, 1987).

[16] Z. You, E.J. Kostelich and J.A. Yorke, *Int. J. Bif. Chaos*, **1** (3) (1991), 605-623.